J. Fluid Mech. (1992), *vol.* 239, *pp.* 523–549
Printed in Great Britain

Effect of boundary reaction on solute dispersion in pulsatile flow through a tube

By BIJOY S. MAZUMDER[1]† AND SAMIR K. DAS[2]

[1] Illinois State Water Survey, University of Illinois at Urbana-Champaign, 2204 Griffith Drive, Champaign, IL 61820, USA

[2] Central Water and Power Research Station, Pune 411024, India

(Received 28 March 1989 and in revised form 14 October 1991)

This paper examines the streamwise dispersion of passive contaminant molecules released in a time-dependent laminar flow through a tube in the presence of boundary absorption or a catalytic wall reaction, which causes a depletion of contaminant in the flow. A finite-difference implicit scheme has been used to solve the unsteady convective–diffusion equation for all time. Here it is shown how the mixing of the cross-sectionally integrated concentration of contaminant molecules is influenced by the frequency of pressure pulsation and the heterogeneous reaction at the boundary. The behaviour of the dispersion coefficient due to the shear effects of steady, oscillatory, and the combined action of steady and periodic currents have been examined separately. The comparison reveals that for all cases the dispersion coefficient asymptotically reaches a stationary state after a certain time and it decreases with the absorption parameter. The increased wall absorption causes negatively skewed deviations from Gaussianity.

1. Introduction

In his classic paper, Taylor (1953) discussed the dispersion of a passive contaminant in a viscous liquid flowing in a circular pipe under laminar conditions. Aris (1956) subsequently presented a method of moment analysis of dispersion in steady flow and discussed the asymptotic behaviour of the second moment about the mean.

Aris (1960) used his method of moments to analyse the longitudinal dispersion coefficient of a solute in an oscillatory flow of a viscous incompressible fluid within an infinite tube under a periodic pressure gradient. However, his analysis of the dispersion coefficient was limited to asymptotically large time after the injection of the solute. An exact solution of the diffusion equation, which was linear in the axial coordinate, was obtained by Chatwin (1975) to study the dispersion of passive contaminant molecules along the axis of the tube, in which flow varied periodically with time. His assumption on linearity of the concentration solution was adequate for large time. Purtell (1981) analysed the effect of flow oscillation (without a time-mean velocity) due to the periodic pressure gradient on the axial diffusion of a solute in a pipe, considering a small perturbation to the oscillation Reynolds number *Re* ($= \omega R^2/\nu$), where ω is the frequency of oscillation, R is the radius of the tube, and ν is the kinematic viscosity of the fluid. His attention was restricted to the initial

---

† Present Address: Mathematics and Statistics Division, Indian Statistical Institute, 203 B.T. Road, Calcutta 700035, India.

distribution of solute, a step function. Smith (1982, 1983*a*) analysed the variance and the longitudinal dispersion coefficient during the initial time in the oscillatory current. He showed that the dispersion coefficient was sometimes negative due to the reversing flow in the velocity profile, which means that the concentration of contaminant may contract and expand periodically; and he also pointed out the sensitivity of time of release of contaminant during a cycle. Yasuda (1984, 1989) presented a method to escape the negative dispersion coefficient during the initial to stationary stages in both steady and oscillatory current by proposing a new definition of the vertical average of the dispersion.

Some important characteristics of time-dependent laminar flows may be found in Jimenez & Sullivan (1984), who studied the growth of rate of variance by using the probabilistic approach proposed by Taylor (1921). Mukherjee & Mazumder (1988) presented an analytical solution for studying the all-time evolution of the central moments of dispersion of passive contaminant molecules in the shearing current due to the combined effect of steady and periodic flows within a conduit of uniform cross-section. They studied the contribution of oscillation of fluid to variance and the longitudinal dispersion coefficient during the initial to stationary stages within a tube, given a uniform initial distribution of contaminant cloud and a large Péclet number. Their analysis was carried out in terms of the combined action of steady flow due to the mean pressure gradient and the unsteady flow due to the imposed perturbation.

Our main objective of the present paper is to explore the effect of absorption or heterogeneous first-order reaction at the boundary on the streamwise dispersion of contaminant cloud released in both steady and oscillatory flows in a tube. More precisely, we study, for all time, how the material spreads due to the shear effect caused by the combined action of flow and diffusion in the cross-sectional plane about its mean position, the speed of the slug's centre of mass, the degree of absorption in the boundary, and the mean concentration distribution's approach to Gaussianity. A numerical scheme (Crank–Nicolson type) has been adopted to study the integral moment equations for all time periods. The mean concentration distribution is approximated by Edgeworth series expansion using the first four central moments, when the contaminant is initially uniform over the cross-section and the Péclet number is large. The results of this study are likely to be of some interest in laminar unsteady flow reactors determining the rates of chemical reaction taking place in the fluid. The significance of the boundary absorption problem can also be thought of as being deposition, transport across a semipermeable membrane, and depletion of pollutants released from the chemical plants. Fischer *et al.* (1979) in particular have drawn attention to the longitudinal dispersion of non-conservative decaying substances, such as biochemical oxygen demand in sewage effluent or heat in a power station discharge.

Gupta & Gupta (1972) studied the phenomenon of dispersion of reactive contaminants in a liquid flowing through a channel in the presence of a first-order heterogeneous chemical reaction using Taylor's (1953) conceptual model for asymptotically large time. Gill, Ruckenstein & Hsieh (1975) explored the generalized dispersion model proposed by Gill & Sankarasubramanian (1970) to study a first-order reaction catalyzed by the wall of a laminar flow tubular reactor, but they confined their analysis to the steady flow and to the case of asymptotic behaviour for large time. Smith (1983*b*) discussed the effect of the boundary reaction on the longitudinal dispersion in shear flows using the delay-diffusion equation. An attempt was made by Barton (1984) to explain the dispersion of reactive contaminants in pipe

Poiseuille flow in the presence of the boundary reaction for asymptotically large time. Purnama (1988) also analysed the case of reaction and retention at flow boundaries when the contaminant is chemically active.

2. Mathematical formulation

Consider an unsteady fully developed viscous, incompressible, axisymmetric laminar flow in a straight circular pipe with uniform cross-section of radius R. The dimensional radial and axial coordinates are r' and z', respectively. The flow is driven by an axial pressure gradient that varies periodically with time. The mean axial pressure gradient $(P_{z'})$ is perturbed by a fluctuation in which the longitudinal pressure gradient $(\partial_{z'} p)$ satisfies the following equation:

$$-\rho^{-1}\partial_{z'}p = P_{z'}(1+\epsilon\,\mathrm{e}^{\mathrm{i}\omega t'}), \quad t' \geqslant 0, \tag{1}$$

where $\epsilon P_{z'}$ and ω are the amplitude and frequency of pressure pulsation, respectively, ρ is the density of fluid, and t' is the time.

The Navier–Stokes equations thus reduce to

$$\partial_{t'}u' = -\rho^{-1}\partial_{z'}p+\nu r'^{-1}\partial_{r'}(p'\partial_{r'})\,u' \tag{2}$$

and the boundary conditions for the flow are

$$u' = 0 \quad \text{at} \quad r' = R \quad \text{and} \quad \partial_{r'}u' = 0 \quad \text{at} \quad r' = 0. \tag{3}$$

Here $u'(t', p')$ is the velocity parallel to the axis $(r' = 0)$ of the tube, which includes both steady and oscillatory parts of the flow, and ν is the kinematic viscosity of the fluid.

When a slug of a reactive solute is released in the above time-dependent flow in a tube with first-order reaction at the wall (assumed to be catalytic), the concentration $C(t,r,z)$ of the reactive solute, with constant molecular diffusivity D, satisfies the dimensionless convective–diffusion equation of the form

$$\partial_t C+Pe\,[u_0(r)+u_1(t,r)]\,\partial_z C = r^{-1}\partial_r(r\partial_r)\,C+\partial_z^2 C, \tag{4}$$

where the dimensionless quantities are given by

$$r = \frac{r'}{R}, \quad z = \frac{z'}{R}, \quad t = \frac{Dt'}{R^2}, \quad u_0 = \frac{u_0'}{U}, \quad u_1 = \frac{u_1'}{U}, \quad Pe = \frac{RU}{D}.$$

Here $u_0(r)$ is the steady velocity, $u_1(t,r)$ the periodic velocity due to the imposed perturbed pressure gradient, U is the reference velocity, and Pe is the Péclet number that measures the relative characteristic times of the diffusion process (R^2/D) to the convective process (R/U). The initial and boundary conditions are

$$\left.\begin{aligned}
&C(0,r,z) = \delta(z),\\
&\partial_r C+\beta C = 0 \quad \text{at} \quad r = 1,\\
&C \text{ finite at all points},\\
&z^m\partial_z^n \to 0 \quad \text{as} \quad |z| \to \infty \quad \text{for} \quad m,n = 0,1,2,\ldots,\\
&\frac{1}{\pi}\int_0^1\int_0^{2\pi}\int_{-\infty}^{\infty} rC(0,r,z)\,\mathrm{d}r\,\mathrm{d}\theta\,\mathrm{d}z = 1,
\end{aligned}\right\} \tag{5}$$

where $\delta(z)$ is the Dirac delta function and $\beta(=\beta' R)$ is the first-order reaction rate parameter corresponding to the catalytic reaction at the wall. The case $\beta = 0$ is usually referred to as the dispersion of passive contaminant that is neutrally buoyant and chemically inert.

The flow velocities $u_0(r)$ and $u_1(t, r)$ in (4) are obtained by solving (1) and (2) subject to the condition (3), given by Sexl (1930) and Uchida (1956) as

$$u(t,r) = u_0(r) + u_1(t,r), \tag{6}$$

where

$$u_0(r) = (1-r^2),$$

$$u_1(t,r) = -\frac{4\mathrm{i}\epsilon}{\alpha}\left[1 - \frac{J_0(r(-\mathrm{i}\alpha)^{\frac{1}{2}})}{J_0(-\mathrm{i}\alpha)^{\frac{1}{2}}}\right]\exp(\mathrm{i}\alpha\, Sc\, t),$$

$u = u'/U$ is the dimensionless axial velocity (U being the time-averaged axial velocity $P_z R^2/4\nu$), $\alpha = \omega R^2/\nu$ is the dimensionless frequency parameter or oscillation Reynolds number, $Sc = \nu/D$ is the Schmidt number, and J_0 denotes the Bessel function of order zero. The first term of right-hand side of (6) represents a 'pipe Poiseuille flow' and the second term corresponds to the unsteady part of the flow (Schlichting 1966). Here, of course, the physical significance is attributed only to the real part. This velocity profile is more general than that assumed by other researchers to study the dispersion process.

Following the method proposed by Aris (1956), we define the pth moment of the distribution of the solute in the filament through r at time t given by

$$C_p(t,r) = \int_{-\infty}^{\infty} z^p C(t,r,z)\,\mathrm{d}z, \tag{7}$$

and the pth moment of the distribution of the solute over the cross-section of the tube

$$M_p(t) = \overline{C}_p = \frac{1}{\pi}\int_0^{2\pi}\mathrm{d}\theta\int_0^1 rC_p(t,r)\,\mathrm{d}r. \tag{8}$$

Multiplying (4) by z^p and integrating with respect to z from $-\infty$ to $+\infty$ with suitable conditions, one gets

$$\partial_t C_p - r^{-1}\partial_r(r\partial_r)C_p = p\,Pe\,u(t,r)\,C_{p-1} + p(p-1)\,C_{p-2}, \tag{9a}$$

$$C_p(0,r) = 1, \quad \partial_r C_p + \beta C_p = 0 \quad \text{at} \quad r = 1. \tag{9b}$$

After integration with respect to r and θ, (9a, b) become

$$\mathrm{d}_t M_p + 2\beta C_p(t, +1) = p\,Pe\,\overline{u(t,r)\,C_{p-1}} + p(p-1)\,\overline{C_{p-2}}, \tag{10a}$$

$$M_p(0) = 1 \quad \text{for} \quad p = 0, \quad M_p(0) = 0 \quad \text{for} \quad p > 0, \tag{10b}$$

where an overbar denotes the cross-sectional mean. The pth integral moment of the concentration distribution can be defined as

$$\nu_p(t) = \frac{\dfrac{1}{\pi}\displaystyle\int_0^{2\pi}\int_0^1\int_{-\infty}^{\infty} r(z-z_g)^p C\,\mathrm{d}r\,\mathrm{d}\theta\,\mathrm{d}z}{\displaystyle\iiint C\,\mathrm{d}v}, \tag{11}$$

where

$$z_g = \frac{\displaystyle\iiint zC\,\mathrm{d}v}{\displaystyle\iiint C\,\mathrm{d}v} = \frac{M_1}{M_0}$$

is the 'centroid' of the cloud and $\iiint C\,\mathrm{d}v = M_0$ represents the total mass of reactive solute in the whole volume of the tube, which decays gradually with time due to the reaction at the wall. The global moments of concentration defined by (11) serve as simple and physically meaningful descriptors of the overall behaviour of the slug. For example, the first moment (z_g) measures the location of the centre of gravity of the slug movement with the mean velocity of the fluid particles, initially located at the source; the second central moment (ν_2) about the mean (z_g) can be related to the dispersion of the slug about its mean position; and the third (ν_3) and fourth central moments (ν_4) respectively measure the symmetry and peakedness of the distribution of the slug about its mean.

The expressions of central moments thus can be obtained from (11) as

$$\nu_2(t) = \frac{M_2}{M_0} - z_g^2, \tag{12a}$$

$$\nu_3(t) = \frac{M_3}{M_0} - 3z_g\,\nu_2 - z_g^3, \tag{12b}$$

$$\nu_4(t) = \frac{M_4}{M_0} - 4z_g\,\nu_3 - 6z_g\,\nu_2 - z_g^4. \tag{12c}$$

The aim of the analysis is to solve the system of differential equations (9) and (10) subject to the given initial and boundary conditions for $p = 0, 1, 2, \ldots$. For a special case ($\beta = 0$ in (9*b*)), the method of solution of the moment equations for a periodic flow was given by Mukherjee & Mazumder (1988) by suitably modifying the treatment of Barton (1983), who studied only a steady current. The solution was based on the method of separation of variables, which depends on a certain eigenvalue problem with a discrete spectrum of eigenvalues. Our method provided an algorithm for the exact analysis of the subsequent central moments, but we restricted our attention only to the variance, that is, the second central moment. The solution was obtained for the combined action of the steady and the periodic currents; and the formal expression for the apparent dispersion coefficient is presented as (see equation 4.8 of Mukherjee & Mazumder 1988)

$$D_\mathrm{a} = \sum_j \left[\frac{16}{\alpha_j^6} + \left\{\frac{A_j}{\alpha_j^2 + \mathrm{i}\alpha Sc} - \frac{4}{\alpha_j^4}\right\}\left\{\frac{4}{\alpha_j^2} - A_j\,\mathrm{e}^{\mathrm{i}\alpha Sct}\right\}\mathrm{e}^{-\alpha_j^2 t} \right.$$
$$\left. - \frac{4(2\alpha_j^2 + \mathrm{i}\alpha Sc)\,A_j\,\mathrm{e}^{\mathrm{i}\alpha Sct}}{\alpha_j^4(\alpha_j^2 + \mathrm{i}\alpha Sc)} + \frac{A_j^2\,\mathrm{e}^{2\mathrm{i}\alpha Sct}}{\alpha_j^2 + \mathrm{i}\alpha Sc}\right], \tag{13}$$

where $$A_j = -8\mathrm{i}\epsilon(-\mathrm{i}\alpha)^{\frac{1}{2}} J_1(-\mathrm{i}\alpha)^{\frac{1}{2}}/\alpha(\alpha_j^2 + \mathrm{i}\alpha)\,J_0(-\mathrm{i}\alpha)^{\frac{1}{2}}.$$

and $\alpha_j, j = 1, 2, \ldots$ are the roots of the Bessel function J_1 of order one. The right-hand side of (13) represents the dispersion coefficients due to the shear effect individually generated by the steady current, the oscillatory current, and the combined action of the steady and oscillatory currents. In the case of steady flow ($\epsilon = 0$) the expression for D_a is in complete agreement with Barton (1983). However, if we ignore the steady flow $u_0(r)$ in the velocity profile (6), then D_a is given by

$$D_\mathrm{a} = \sum_j A_j^2\,(\mathrm{e}^{2\mathrm{i}\alpha Sct} - \mathrm{e}^{(\mathrm{i}\alpha Sc - \alpha_j^2)t})/(\alpha_j^2 + \mathrm{i}\alpha Sc), \tag{14}$$

which is only for the shear effect due to the oscillatory current. The dispersion coefficient due to the periodic current was not studied separately by Mukherjee &

Mazumder (1988). This result is consistent with the work of Chatwin (1975) for asymptotically large time after the release.

3. Numerical scheme

Owing to the complexity of analytical solutions of moment equations (9*a*) subject to the initial and boundary conditions (9*b*) for $\beta \neq 0$, a finite-difference scheme has been adopted to study the dispersion phenomena. This scheme, essentially based on the Crank–Nicholson implicit approach, was considered not to have the stability limitations of other implicit schemes (Lapidus & Pinder 1982). For a consistent set of initial information along the radial direction, (9*a*) can be used to 'march' in time to obtain the evolving mean concentration field. The finite-difference formulation of the above equations is similar to the scheme used by Mazumder & Das (1989). They applied an implicit two-level time integration scheme with second-order accuracy in the marching direction and a third-order accuracy along the radial direction. In particular, the derivatives in the marching direction have been replaced by a backward difference. Central differencing is used in all derivatives in the radial direction and then the resulting difference scheme is implicit. The finite-difference representation of derivatives and the various terms can be written at mesh points $(i+1,j)$ where $i=0$ corresponds to the time $t=0$, and $j=0$ corresponds to the axis of the pipe, $r=0$. The resulting finite-difference equations become simultaneous linear algebraic equations with a tridiagonal coefficient matrix:

$$P_j C_p(i+1,j+1)+Q_j C_p(i+1,j)+R_j C_p(i+1,j-1)=S_j, \tag{15}$$

where P_j, Q_j, R_j, and S_j are the matrix elements and $i+1, j$ are the indices at the grid point considered. The tridiagonal coefficient matrix arising from (15) can be solved by the well-known method of the Thomas algorithm, which is basically a variation of Gaussian elimination (Anderson, Tannehill & Pletcher 1984). When applied to the system, the Thomas algorithm necessitates an iteration procedure and the resulting difference equation here is backward. It is clear that the system of algebraic equations is readily solved provided the initial and boundary conditions are specified. The finite-difference analogues of the entry and boundary conditions (9*b*) are

$$\left.\begin{aligned} C_p(1,j) &= \begin{cases} 1 & \text{for} \quad p=0 \\ 0 & \text{for} \quad p \geqslant 1, \end{cases} \\ C_p(i+1,1) &= C_p(i+1,-1) \end{aligned}\right\} \tag{16}$$

at the axis, and

$$\frac{1}{2\Delta r}[C_p(i+1,N+1)-C_p(i+1,N-1)]+\beta C_p(i+1,N)=0 \tag{17}$$

at the boundary for $p \geqslant 0$.

To integrate (10*a*), we employ Simpson's one-third rule on the right-hand side, considering the radius of the pipe as a ten-layer model. The steps of computations are as follows: the time-dependent axial velocity u is computed from (6); the concentration C_p is calculated on knowing the values of u at grid point $(i+1,j)$; finally, M_p is computed from (10*a*) and (10*b*) after substituting the values of u and C_p in the corresponding grid point. The above procedure is followed recursively in the marching direction. Numerical experimentation has been done for three different velocity profiles to separate the individual dispersion processes due to the steady, the periodic and, for comparison, the combined effect of the steady and periodic currents.

For the steady current, a mesh size ($\Delta t = 0.0001$, $\Delta r = 0.1$) gives satisfactory results when checked for accuracy by repeating the computations for smaller mesh sizes. The present scheme is linearly stable for a finite value of n, where $n = \Delta t/(\Delta r)^2 = 0.01$, because of its implicit character. For the oscillatory current, a mesh size ($\Delta t = 0.00001$, $\Delta r = 0.1$) gives results for frequency parameter $\alpha = 0.5, 1.0$, and 4.0. The value of n is 0.001. In particular, for $\alpha = 1.0$ and 4.0, the smaller time interval is needed to obtain the oscillatory behaviour in the dispersion process. For the combined effect of steady and oscillatory currents a mesh size ($\Delta t = 0.00001$, $\Delta r = 0.1$) gives satisfactory results for $\epsilon = 1.5$, and $\alpha = 0.5, 1.0$, and 4.0. The value of n is 0.001.

4. Discussion of integral moments

A numerical check was made on the integral moments (variance, skewness) of the concentration distribution and the longitudinal dispersion coefficient for the steady flow $[u = u_0(r),\ u_1(t,r) = 0]$ in the absence of boundary absorption or chemical reaction ($\beta = 0$). The results are in good agreement with those of Gill & Sankarasubramanian (1970), Barton (1983), Barton & Stokes (1986), and Mukherjee & Mazumder (1988).

When $p = 0$, the solution of (10*a*) subject to (10*b*) is given by

$$M_0(t,\beta) = 1-2\beta\int C_0(t,\ +1)\,\mathrm{d}t, \tag{18}$$

where $C_0(t,\ +1)$ is found from (9*a*). Equation (18) represents the total mass of reactive solute, which is a function of β and t. Figure 1 shows how the total amount of reactive material is depleted over time for a given reaction parameter β. When $\beta = 0$, $M_0(t,0) = 1$, which represents a constant mass. As expected, dimensionless mass $M_0(t,\beta)/M_0(\beta = 0)$ is a decreasing function of β and t.

For $p = 1$, (10*a*) and (10*b*) can be written as

$$\left.\begin{aligned} \mathrm{d}_t M_1 + 2\beta C_1(t,\ +1) &= Pe\overline{[u_0(r)+u_1(t,r)]\,C_0},\\ M_1(0) &= 0. \end{aligned}\right\} \tag{19}$$

We focus our attention on the overall transport rate of contaminant molecules, the mean longitudinal displacement (z_g) of the dispersive material moving with the mean velocity of the fluid particles have been presented separately for steady, periodic and the combined action of steady and periodic currents.

Figure 2 shows the centroid displacement (z_g) for $\beta = 0, 1, 3, 5$, and 10. For a given β, it is observed that the centroid displacement (z_g) increases linearly with time and it advances for a given time t, and the mean position of material moves more rapidly than the average velocity $\bar{u}_0$, when the reaction takes place. Figure 3 (*a*, *b*) shows the first moment (z_g) for $\alpha = 1.0$, which measures the centre of gravity of the slug moving cyclically with the same frequency as the oscillatory current. The amplitude of oscillation increases with the boundary reaction β; that is, the mean displacement of the slug increases with each complete period of oscillation. The relative mean longitudinal displacement, $z_g/[z_g(\beta = 0)]-1$, for the combined effect of steady and oscillatory currents ($u_0(r)+u_1(t,r)$) increases directly up to a certain period of time, then it moves asymptotically to a constant value (figures 4*a*, *b*). This phenomenon may be explained by the boundary absorption causing the centre of the slug to move with a higher velocity. Within a given time, however, the movement of the centre of the slug is directly proportional to the boundary absorption. Figure 5 shows the

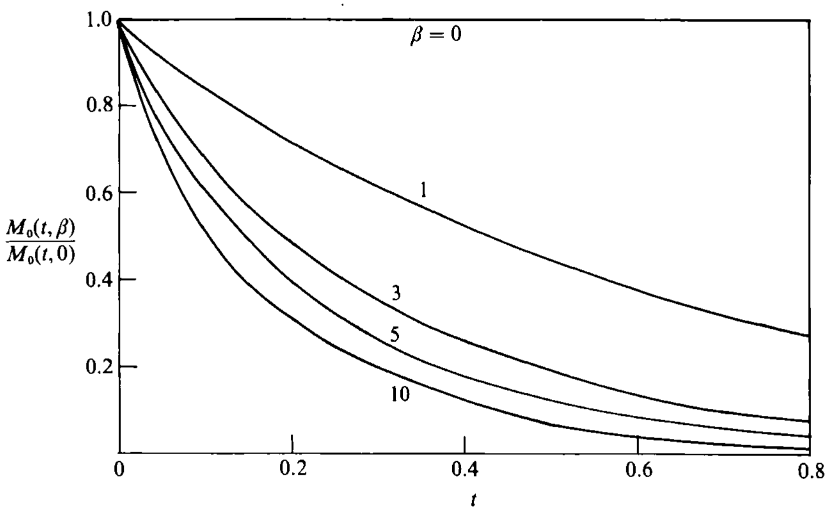

FIGURE 1. Fraction of total slug retained in the flow.

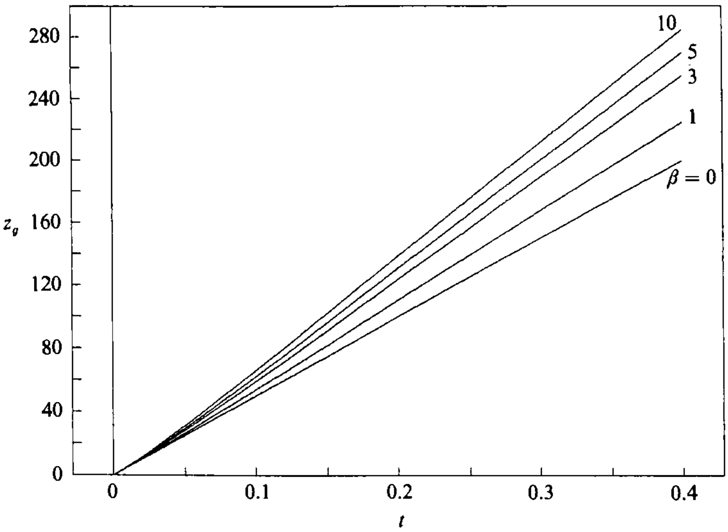

FIGURE 2. The centroid displacement (z_g) as a function of time t for the steady flow, when $Pe = 10^3$.

temporal variation of deposition or absorption (mass/length) at the boundary for various values of β, and $\alpha = 1.0$. The absorption (mass/length) at the boundary can be expressed as

$$\frac{M_0(t_i)-M_0(t_{i+1})}{z_g(t_{i+1})-z_g(t_i)}, \tag{20}$$

where $M_0(t_i)$ and $z_g(t_i)$ respectively represent the total mass and the mean displacement of the slug at the ith time period.

Figure 6 (a–c) presents plots of the variance ($\ln \nu_2$) of the longitudinal concentration distribution against the dispersion time ($\ln t$) for $\alpha = 0.5$, 1.0, and 4.0 and $\beta = 0$, 3, and 10, when $\epsilon = 1.5$, and $Sc = Pe = 10^3$. It is seen from (9a)–(12a) that the second central moment (ν_2) is essentially based on the dispersion due both to the

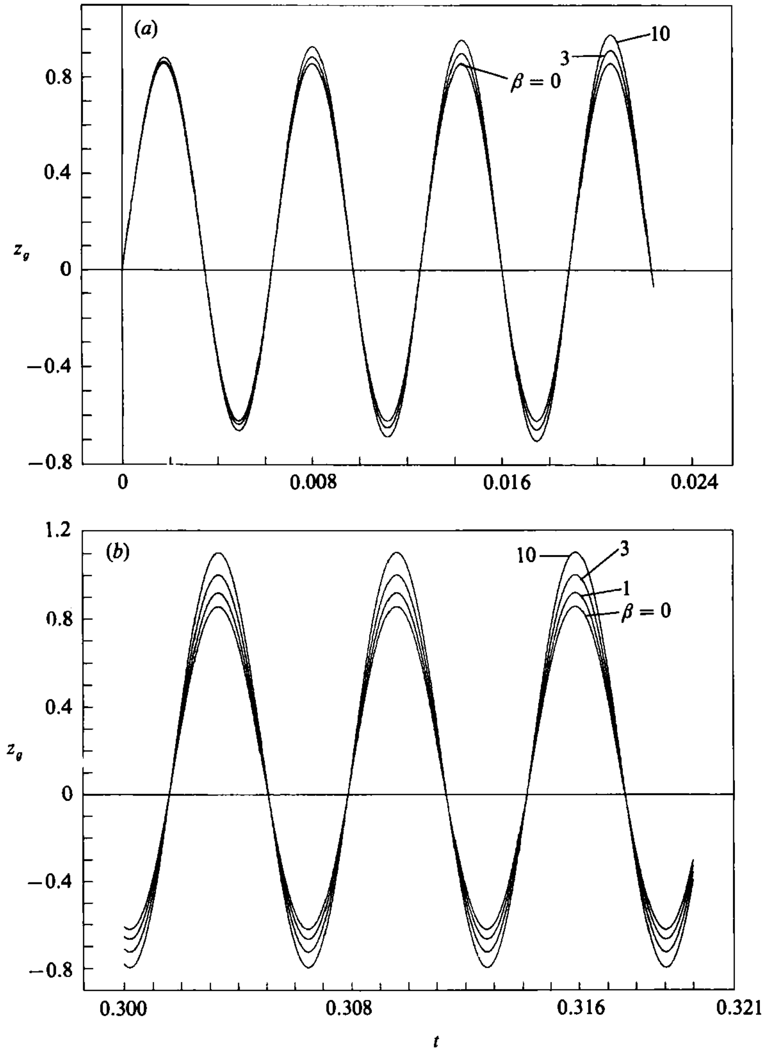

FIGURE 3. The centroid displacement (z_g) due to the periodic flow, when $Pe = Sc = 10^3$, $\alpha = 1.0$: (*a*) small time, (*b*) large time.

longitudinal diffusion and to the interaction of current and lateral diffusion. Figures show that for a given value of β, $\ln \nu_2$ increases rapidly with time. At low frequency, $\ln \nu_2$ increases in a wavy way, whereas at high frequency there is no such effect. The shear effect due to a periodic flow is small compared with that of a steady flow. Again, for fixed α, variance decreases with β, which reflects the combined effects of the lateral distribution of the remaining concentration and the velocity.

Aris (1956) showed in his simplified model that for asymptotically large time the rate of growth of variance of the distribution of the solute in a steady flow through a tube is proportional to the sum of the molecular diffusion coefficient D and the apparent diffusion coefficient $U^2R^2/48D$, where U is the average velocity. According to Aris, the rate of growth of variance $\nu_2(t)$, for the present case, can be written as

$$\frac{\mathrm{d}\nu_2}{\mathrm{d}t} = 2 + 2Pe^2 D_a(Sc, \epsilon, \alpha, \beta, t), \tag{21}$$

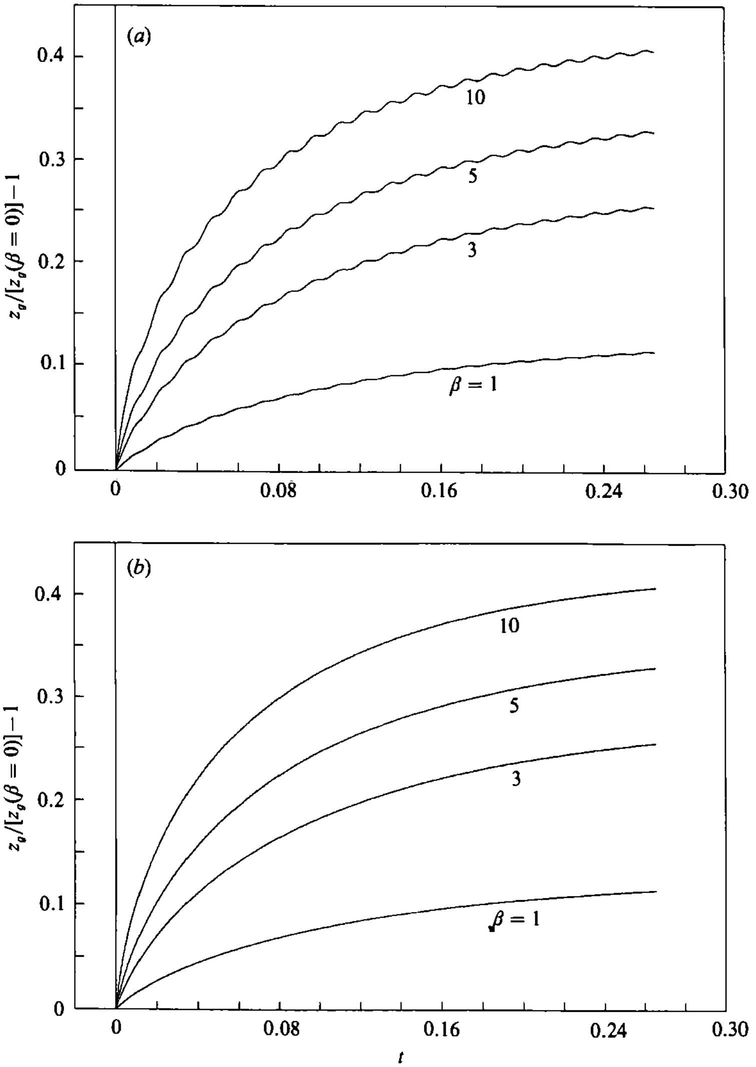

FIGURE 4. The relative mean displacement due to the combined shear effects (steady and unsteady) against time t for $Pe = Sc = 10^3$, $\epsilon = 1.5$: (a) $\alpha = 0.5$, (b) $\alpha = 4.0$.

where $D_{\rm a}(\ldots)$ is the apparent diffusion coefficient. The first term of the right-hand side of (21) represents the longitudinal diffusion, and the second term represents the interaction between the convection and lateral diffusion. As the first term does not affect the convection, only the apparent dispersion coefficient is discussed for each velocity profile (steady, oscillatory, and the combined effect of steady and periodic currents that flow in the same direction).

When the flow is steady, $D_{\rm a}$ is a function only of β and t. The dispersion coefficient $D_{\rm a}$ for steady current $u_0(r)$ initially increases and asymptotically reaches a steady state (~ 0.005) at dimensionless time $t \approx 0.3$. For a given time t, $D_{\rm a}$ decreases with the boundary absorption.

For the oscillatory current $u_1(t, r)$, $D_{\rm a}$ mainly depends on the frequency of oscillation α, the Schmidt number Sc, the dispersion time t, and the absorption parameter β. Now $\alpha = \omega R^2/\nu = 2\pi(R^2/\nu)/T$, which is a measure of the ratio of the

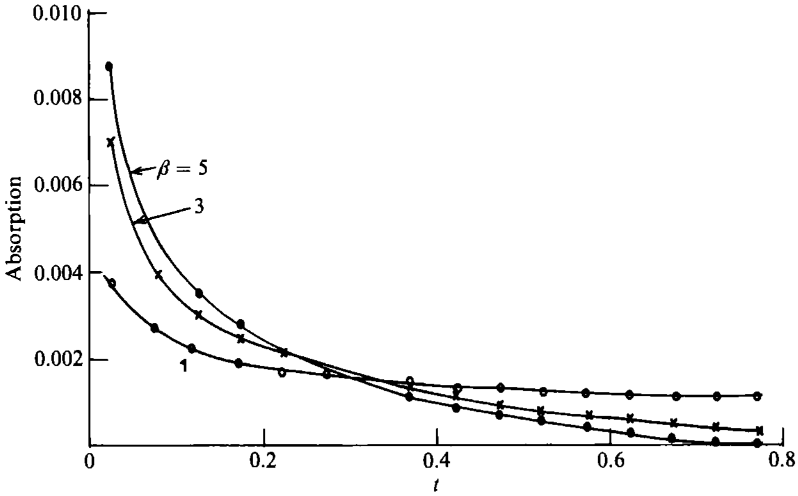

FIGURE 5. Deposition (mass/length) at the boundary due to combined shear effects for $\epsilon = 1.5$, $\alpha = 1.0$.

time (R^2/ν) taken for viscosity to smooth out the transverse variation in vorticity to the period of oscillation $(1/\omega)$, or the ratio of the pipe radius R to the Stokes-layer thickness $(\nu/\omega)^{\frac{1}{2}}$. A small value of α implies a large viscous layer near the wall compared with a small inviscid core near the centre or, alternatively, a large oscillation period compared with viscous diffusion time and therefore quasi-steady flow, and vice versa for large α. The Schmidt number $Sc(=\nu/D)$ is the ratio of viscous diffusion and molecular diffusion; and $\alpha Sc = (R^2/D)\,2\pi/T$, is a measure of the ratio of the characteristic time of transverse diffusion to the period of oscillation. The variations of D_a with time in the oscillatory current $u_1(t,r)$ are plotted for various values of β and $Sc = 1000$ in figure 7 for $\alpha = 0.5$, figure 8 for $\alpha = 1.0$ and figure 9 for $\alpha = 4.0$. In this paper, values of the characteristic transverse mixing time ratio $(T_r = \alpha Sc/2\pi)$ for low, medium, and high frequencies are derived as 80, 159, and 637, respectively. From the figures, it can be seen that D_a in the oscillatory flow changes cyclically with a double-frequency period, and it reaches a stationary state after a certain time t, which is related to the cross-sectional mixing time R^2/D. In the case of low frequency, D_a reaches a stationary state earlier than for high frequency. The amplitudes of oscillation of D_a during the first and second half of the period of oscillatory flow are approximately equal. But in the case of high frequency, the period of oscillation is so short that D_a initially varies almost cyclically with the same frequency as the periodic current and then fluctuates with a double frequency. The longitudinal dispersion coefficient is more significant during the first half of the period than the second one. However, this situation completely stabilizes after a certain time $(t > 0.3)$ and then with oscillation the solute disperses at a fairly uniform rate.

The dispersion coefficient D_a changes cyclically with time even in the stationary state (Yasuda 1984). From these studies, D_a in the oscillatory current was found to be much smaller than D_a in the steady current. According to the work on longitudinal dispersion in an oscillatory current, the shear effect due to the periodic flow becomes asymptotically smaller than that of a steady current when the characteristic time of lateral diffusion is much larger than the period of oscillatory current (Okubo 1967; Holley, Harleman & Fischer 1970). It may also be noted that D_a decreases with the

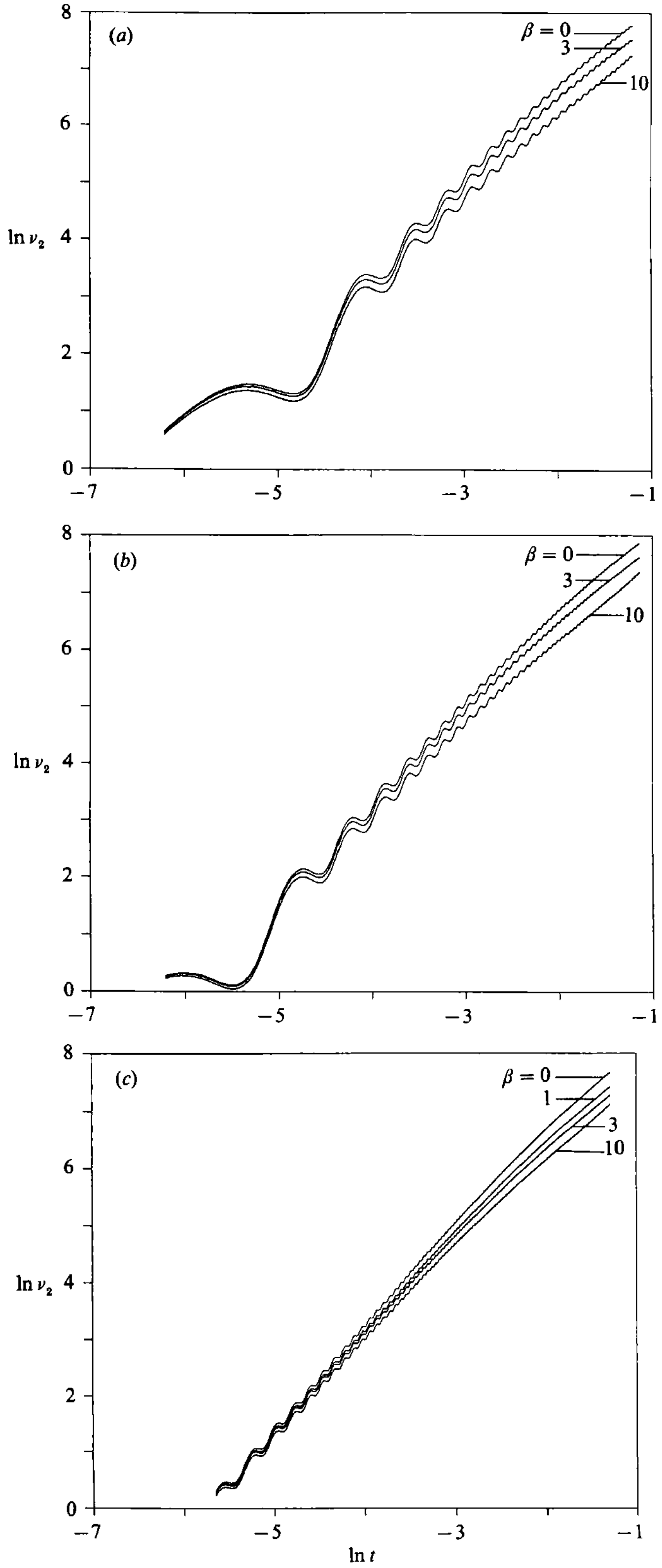

FIGURE 6. The temporal variation of variance of concentration distribution due to combined shear effects for $\epsilon = 1.5$, $Pe = Sc = 10^3$: (*a*) $\alpha = 0.5$, (*b*) $\alpha = 1$, (*c*) $\alpha = 4$.

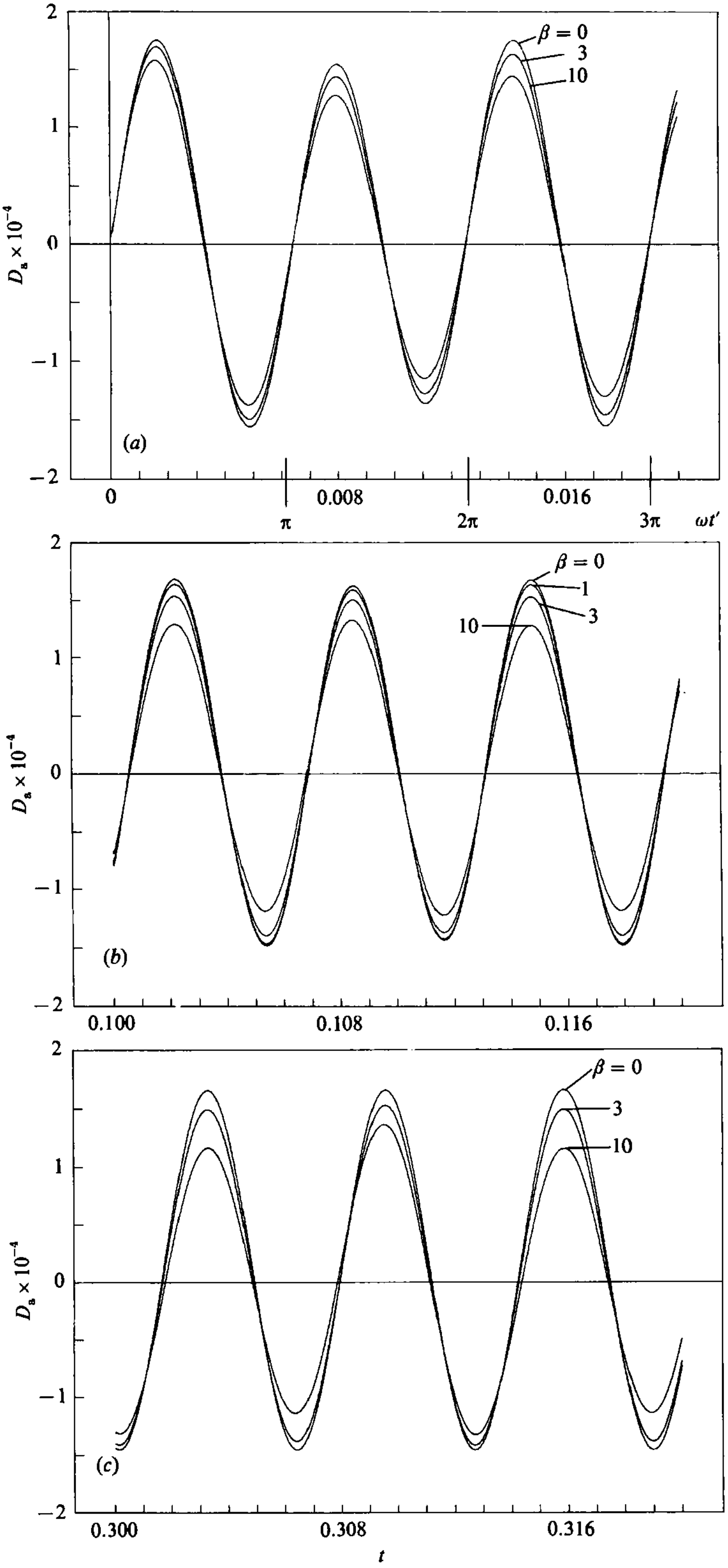

FIGURE 7. The dispersion coefficient D_a due to periodic flow for (*a*) small time, (*b*) medium time, and (*c*) large time, when $Pe = Sc = 10^3$, $\alpha = 0.5$.

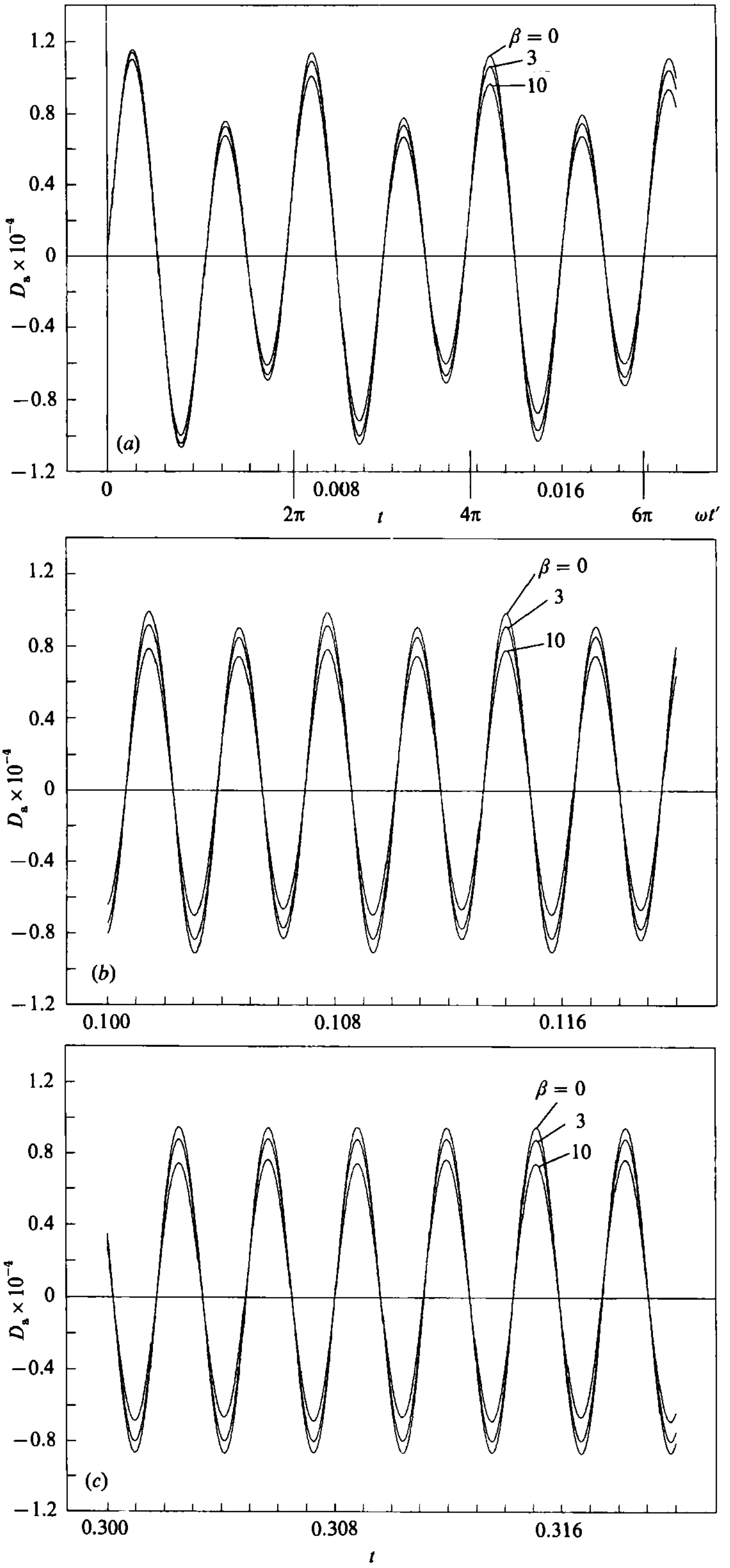

FIGURE 8. As figure 7 but for $\alpha = 1$.

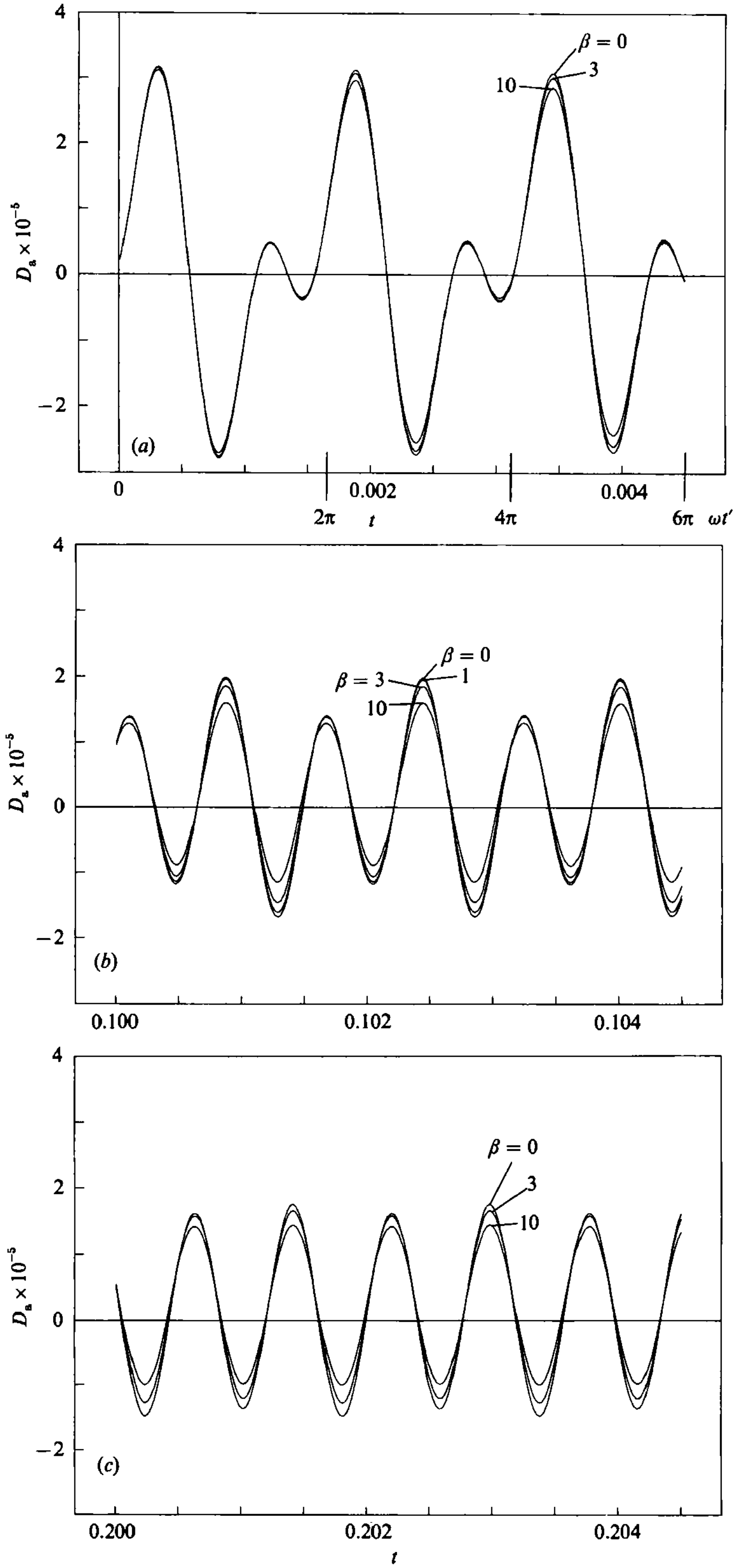

FIGURE 9. As figure 7 but for $\alpha = 4$.

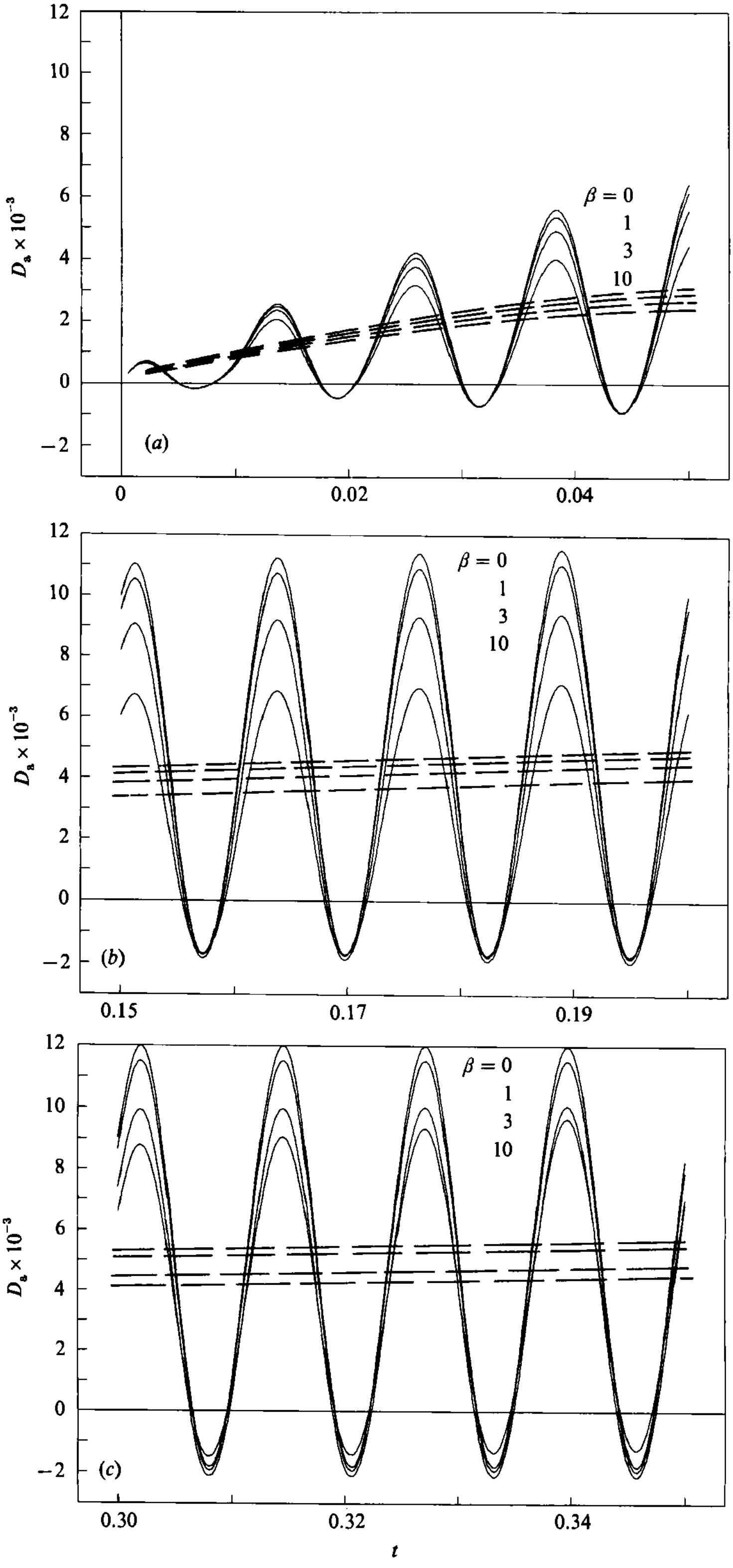

FIGURE 10. The dispersion coefficient D_a and average dispersion coefficient $\overline{D_a}$ (----) due to combined steady and periodic currents for $\epsilon = 1.5$, $\alpha = 0.5$, $Pe = Sc = 10^3$: (a) small time, (b) medium time, and (c) large time.

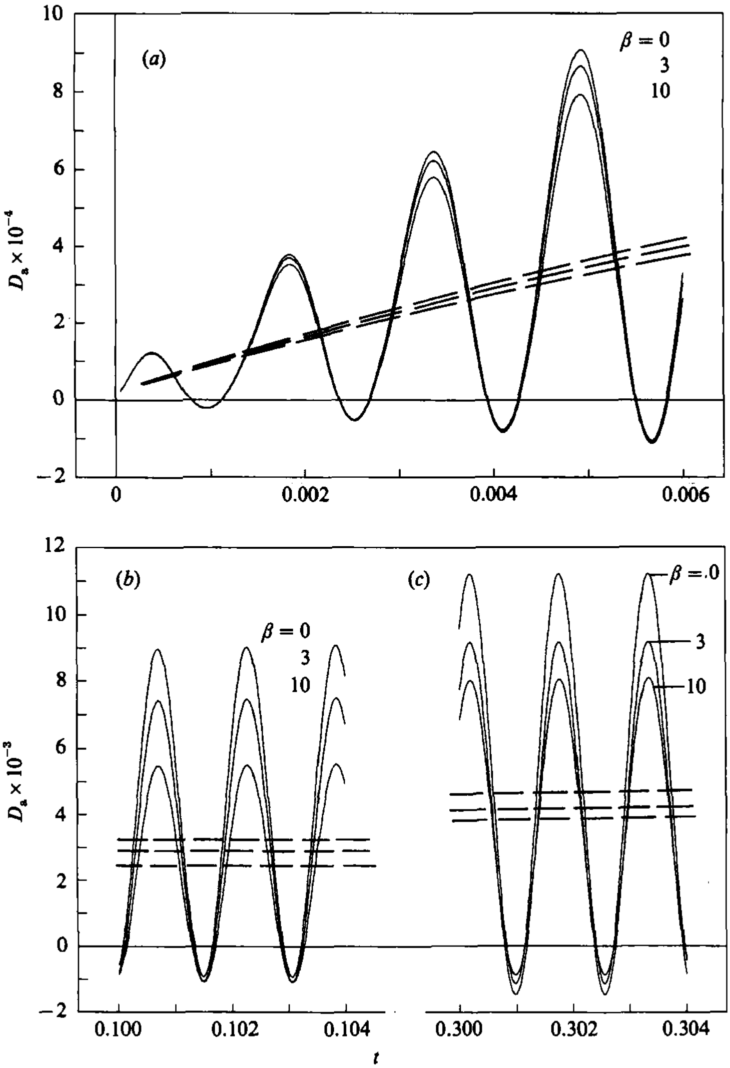

FIGURE 11. As figure 10 but for $\alpha = 4$.

frequency α; that is, the shear effect due to high frequency of the oscillatory current on D_a is negligible, but is more pronounced on the steady current or quasi-steady current. The fluctuations in the velocity profiles induce the positive and negative dispersion during the period of oscillation: owing to the flow reversal in the period, the material would be carried back with the flow to form the negative dispersion. Therefore, the dispersion of material contracts at each flow reversal during the period of oscillation (Smith 1982). Further, the dispersion coefficient D_a for a given frequency of oscillatory current decreases with increases in reaction parameter β.

For comparison, the combined shearing effect of steady and oscillatory currents $(u_0 + u_1)$ on D_a have also been studied for $\epsilon = 1.5, \alpha = 0.5$, and 4.0, and $\beta = 0, 1, 3$, and 10. Figures 10 and 11 show the temporal variation of D_a due to the combined shear effects for low and high frequencies of the oscillatory flow. When these are compared with D_a due to the shear effect of a periodic current, D_a no longer has the double-frequency period. In fact, the amplitude of oscillation increases initially up to certain

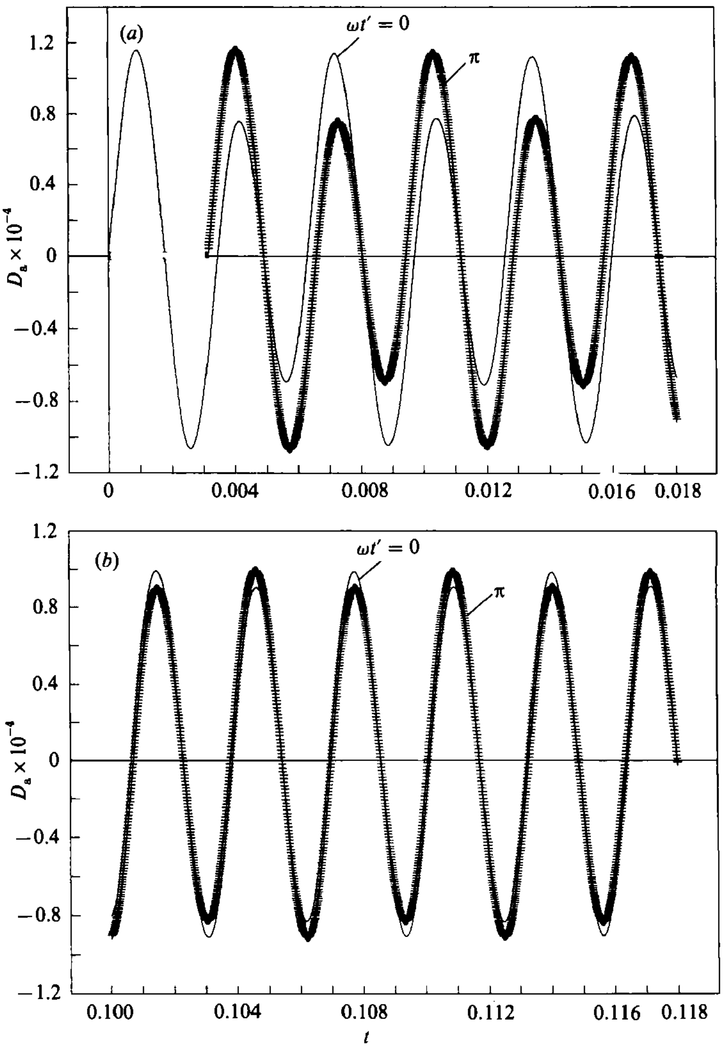

FIGURE 12. The dispersion coefficient D_a for $\beta = 0$, $\alpha = 1.0$: (a) small time, (b) medium time.

time, and then becomes stable for a long time, which means that D_a due to the steady flow plays a more significant role than D_a due to the oscillatory flow. As the periodic flow moves with the steady flow in the same direction, the effect of frequency of oscillation of the periodic current (due to the perturbed pressure gradient) becomes less significant. It follows that just after the injection of reactive material, it tends to disperse longitudinally at a rate which increases with time. This oscillatory nature of D_a makes it worthwhile to concentrate on the averaged longitudinal dispersion coefficient ($\bar{D}_a$) over a period of oscillation (t_i, t_{i+1}) where

$$\bar{D}_a = \frac{1}{t_{i+1} - t_i} \int_{t_i}^{t_{i+1}} D_a(\ldots)\,\mathrm{d}t. \tag{22}$$

For a given frequency of oscillation α, $\bar{D}_a$ is always positive for all values of β (figures 10 and 11). For a given value of α, D_a decreases with increase in β for all cases. Thus, one would expect from the physical point of view that the increase in β leads to an

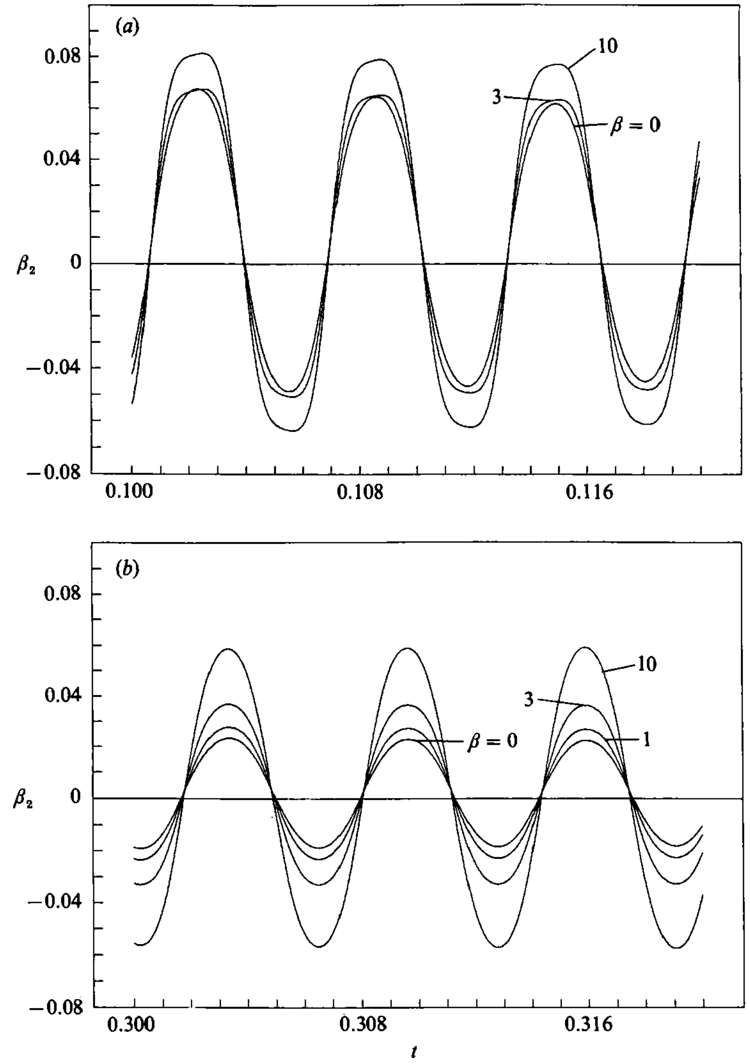

FIGURE 13. The skewness coefficient (β_2) of the concentration distribution due to oscillatory flow for $Pe = Sc = 10^3$, $\alpha = 1.0$.

increasing number of moles of reactive material undergoing chemical reaction or absorption and changing the concentration distribution across the tube; and hence there is a drop in D_a. The decrease of D_a with boundary absorption β corresponds to the increase of D_a due to the boundary retention. The dispersion coefficient is larger when the partial amount of material is in the dead zone region and smaller when it is being is depleted due to the boundary absorption (Valentine & Wood 1977). Further, it may be pointed out (Yasuda 1989) that the decrease of dispersion coefficient D_a corresponds to the increase of dispersion coefficient of suspended particles with the settling velocity.

The analysis has also been performed for the time of cloud discharge taking place at different phases ($\alpha Sc\, t = 0, \frac{1}{3}\pi$, $\frac{2}{3}\pi$ and π). Figure 12(*a*, *b*) shows the temporal variation of D_a for $\alpha = 1.0$, $\beta = 0$ and $\alpha Sc\, t = \omega t' = 0$ and π. It is important to note that although the time of discharge is different, eventually the dispersion coefficients asymptotically coincide with each other (Smith 1983*a*).

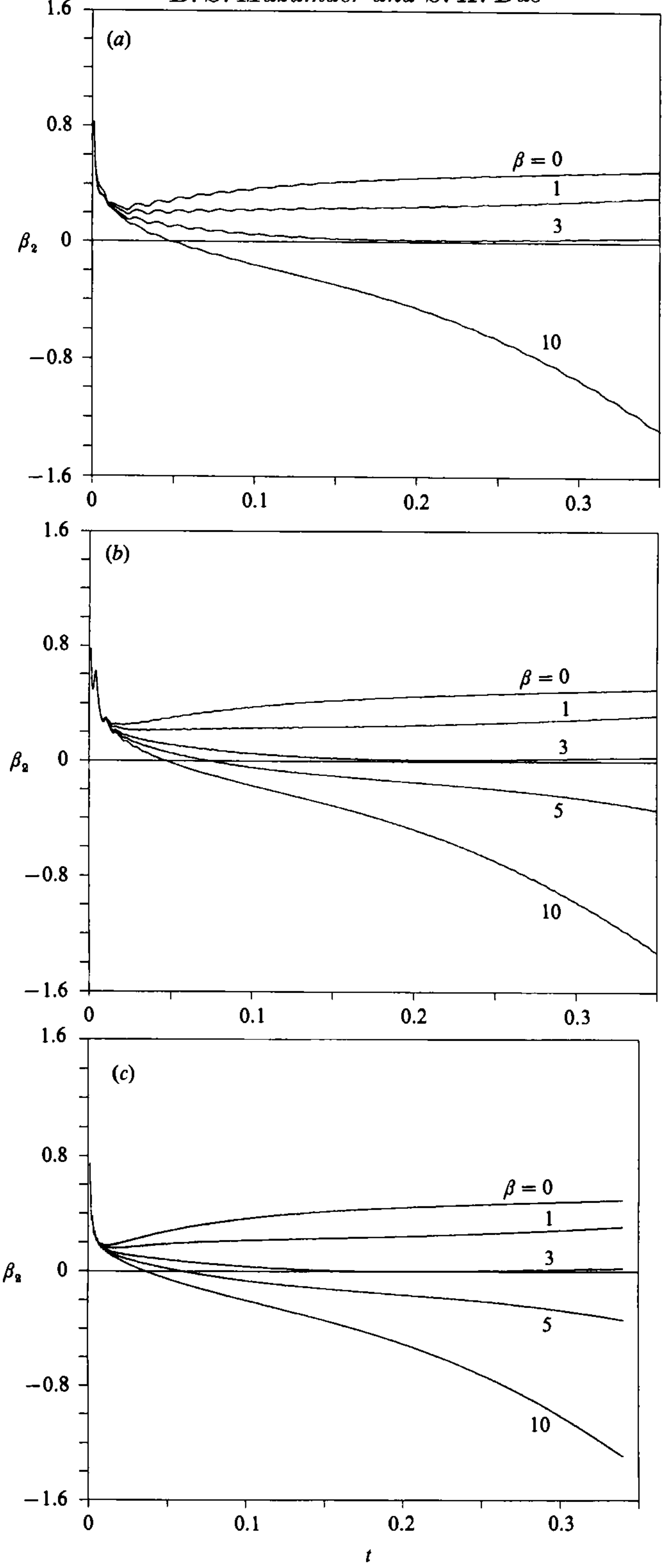

FIGURE 14. The skewness coefficient due to combined shear effects for $\epsilon = 1.5$, $Pe = Sc = 10^3$: (a) $\alpha = 0.5$, (b) $\alpha = 1$, (c) $\alpha = 4$.

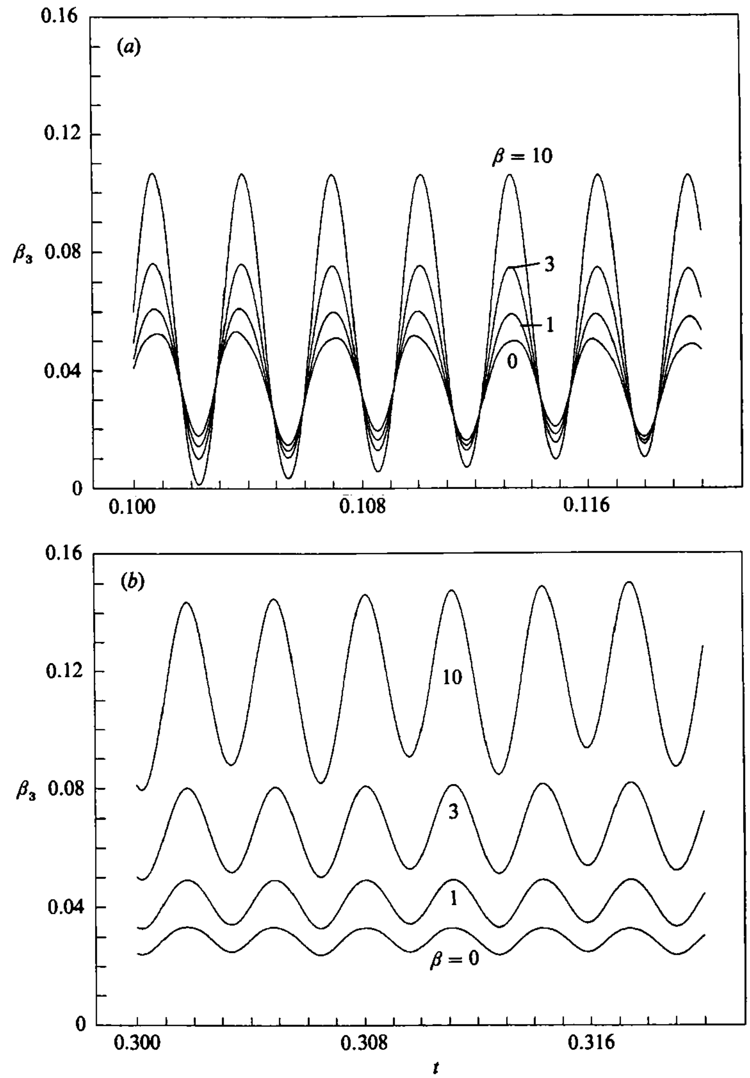

FIGURE 15. As figure 13 but for the kurtosis coefficient (β_3).

The coefficients of skewness (β_2) and kurtosis (β_3) are the important criteria to measure the degree of symmetry and peakedness, respectively, of the concentration distribution. They are used to examine the deviations from Gaussianity. If the concentration distributions are exactly Gaussian, both coefficients will be zero and can be defined as follows:

$$\beta_2 = \nu_3/\nu_2^{\frac{3}{2}} \quad \text{and} \quad \beta_3 = \nu_4/\nu_2^2 - 3. \tag{23}$$

Figure 13(a, b) shows the temporal variation of the coefficient of skewness β_2 for $\alpha = 1.0$ and various values of β. It can be seen that the coefficient of β_2 in the oscillatory current changes cyclically with a single-frequency period and decreases with time t. In a complete period of oscillatory current, β_2 is approximately zero, and hence the concentration distribution is essentially symmetrical. During one half-period of oscillation, the skewness increases with β. Figure 14(a–c) shows the temporal variation of β_2 due to the shear effect of the combined steady and oscillatory flows. It can be seen that initially skewness decreases with time, moves asymptotically to a constant value, and is almost zero for $\beta = 3$; whereas for $\beta > 3$, skewness changes from positive to negative. For $\beta = 3$, the concentration distribution is almost symmetrical after a time $t > 0.2$ for any value of α. It may also be noted that the symmetrical distribution of concentration in the case of an oscillatory current is obtained earlier than for a steady current. For each value of $\beta > 3$, there is a critical time t_c for which skewness is zero; and it is interesting to note that as β increases, t_c decreases. Whether skewness is positive or negative depends on the relative velocity and the remaining slug across the tube. Since the effect of wall reaction causes a depletion of contaminant in the lower-velocity region near the wall, most of the contaminant will remain in the central region of higher velocity. Thus, the small amount of contaminant near the lower-velocity region remains behind to form an extended tail (see Sankarasubramanian & Gill 1973 and Smith 1983*b* for steady flow); whereas in the absence of the boundary reaction, there is a forward tail, or positive skewness (see Taylor 1953; Gill & Ananthakrishnan, 1967; Mazumder & Das 1989 for steady flow).

The temporal variation of the coefficient of kurtosis (β_3) for the periodic current is shown in figure 15(*a*, *b*) and is compared with that of the combined effect of the steady and oscillatory currents. In the oscillatory current β_3 is seen to vary in an oscillatory manner with the double-frequency period. Figure 16(*a*–*c*) shows β_3 against t for various values of α and β. It is seen for the low boundary reaction β_3 is always negative, which represents a leptokurtic distribution. For a large reaction parameter, β_3 changes from negative to positive, and there is a certain time for which the distribution is normal before becoming platykurtic. Therefore, the comparison reveals that the coefficient of kurtosis of the distribution of concentration for the oscillatory flow is much smaller than that for the steady current or the combined steady and periodic currents; and hence the distribution may become Gaussian earlier for the oscillatory than the steady current.

5. Mean concentration distribution

If we can find few central moments of the concentration distribution, it is possible to approximate the mean concentration distribution $C_m(t,z)$ within the tube using Hermite polynomials to represent non-Gaussian curves (Chatwin 1970; Mehta, Merson & McCoy 1974; and Güven, Molz & Melville 1984). The cross-sectional mean concentration $C_m(t,z)$ is defined as

$$C_m(t,z) = M_0(t)\,\mathrm{e}^{-x^2} \sum_{n=0}^{\infty} a_n(t)\,H_n(x), \tag{24}$$

where
$$M_0(t) = \iiint C\,\mathrm{d}v, \quad x = \frac{z-z_g}{(2\nu_2)^{\frac{1}{2}}},$$

and H_i, the Hermite polynomials, satisfy the recurrence relation with $H_0(x) = 1$ as

$$H_{i+1}(x) = 2xH_i(x) - 2iH_{i-1}(x), \quad i = 0, 1, 2, \dots. \tag{25}$$

The coefficients a_i are

$$a_0 = 1/(2\pi\,\nu_2)^{\frac{1}{2}}, \quad a_1 = 0, \quad a_2 = 0, \quad a_3 = 2^{\frac{1}{2}}a_0\,\beta_2/24, \quad a_4 = a_0\,\beta_3/96, \tag{26}$$

The mean concentration distributions $C_m(t,z)$ are plotted against the axial distance $(z-z_g)$ for the combined action of the steady and oscillatory currents in

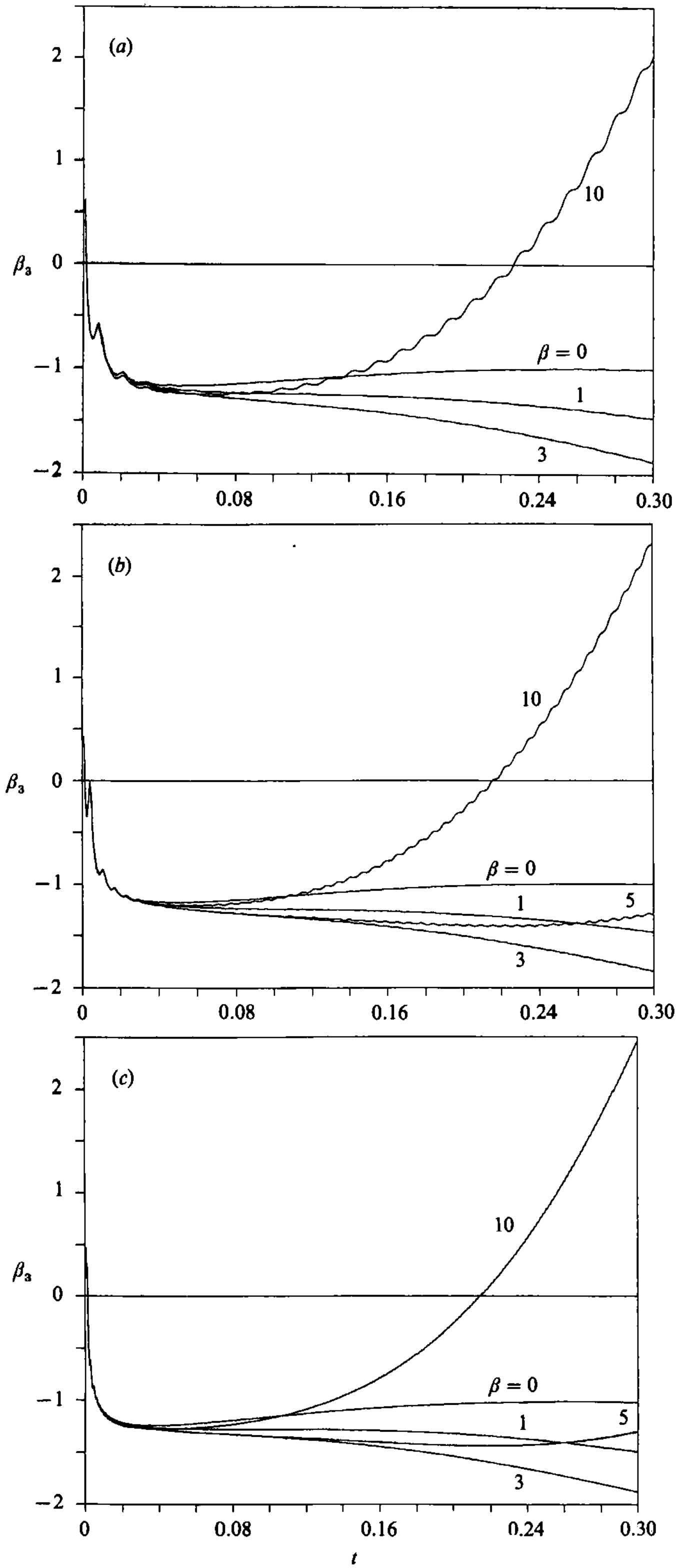

FIGURE 16. As figure 14 but for the kurtosis coefficient.

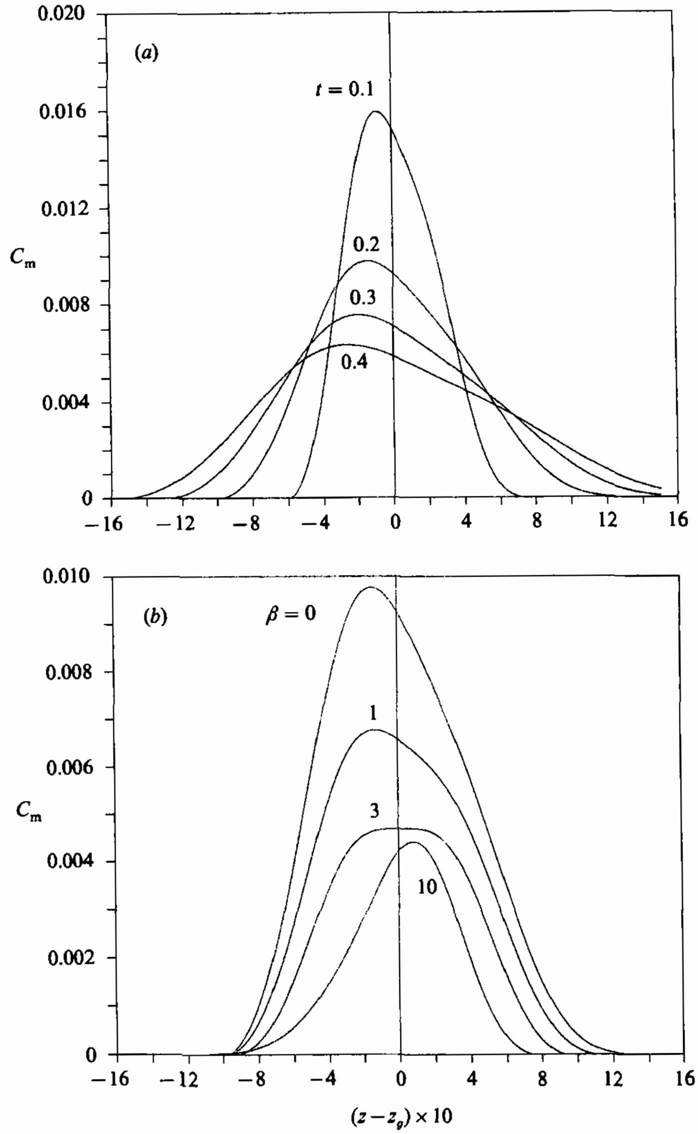

FIGURE 17. The mean concentration distribution along the tube for $\alpha = 1$, $\epsilon = 1.5$, $Pe = Sc = 10^3$; (a) $\beta = 0$ and (b) $t = 0.2$.

figure 17 (*a*, *b*) for various values of β and t. From figure 17 (*a*) it can be seen that for fixed α and $\beta = 0$, the contaminant always remains constant and disperses longitudinally with time. As the dispersion time increases, the peak of the distribution decreases and the distribution tends to become flat. Figure 17 (*b*) shows the depletion of contaminant due to boundary absorption for a given time. For moderate $\beta \sim 3$, the distribution becomes symmetrical at time $t > 0.15$ (also see figure 14), whereas for large $\beta > 3$, it deviates from Gaussianity with a negatively extended tail. It is important to note that the mean longitudinal concentration distribution for the oscillatory flow becomes symmetrical even earlier than that of steady flow. The coefficients of skewness and kurtosis of the concentration distribution in the case of periodic flow are significantly lower than these coefficients for other flows. For steady flow ($\epsilon = 0, \beta = 0$), the profiles of $C_m(t, z)$ along the axis of the pipe agree qualitatively with those given by Chatwin (1970) and Andersson & Berglin (1981) although the forms of $C_{\mathrm{m}}(t, z)$ and the dimensionless axial coordinate defined by them differ markedly from ours. The above observations show a remarkable similarity between the mean concentration distributions due to boundary absorption in the combined shearing–current and due to the steady Poiseuille flow discussed by Barton (1984).

6. Conclusions

We have presented a numerical solution to study the effect of boundary absorption of contaminant molecules on the shear effect due to steady, periodic, and combined steady and periodic currents through a tube; and we have compared some specific results due to different shear effects with particular emphasis on the role played by the first-order reaction at the wall. In particular, computations of higher integral moments C_p $(p = 2, 3, 4, \ldots)$ have been done to better understand the behaviour of the dispersion process over time. All the investigations have been done for flow velocities when the slug of reactive solute is released at maximum pressure at $t = 0$, given an initially uniform slug over the cross-section of the tube and a large Péclet number. The analysis has also been made for the time of release of the slug at different phases $(0, \frac{1}{3}\pi, \frac{2}{3}\pi$, and $\pi)$ and shows that the time of release is important at the initial stage but eventually the dispersion coefficients coincide with each other.

Owing to boundary absorption, the amount of the slug retained in suspension decreases exponentially with dispersion time t, whereas the relative mean displacement of the slug increases immediately after the release up to a certain time, then it moves asymptotically to a constant value.

The apparent dispersion coefficient D_{a} reaches a stationary state in both steady and oscillatory currents over time. For high frequency of the periodic current, it appears that D_{a} varies cyclically with almost the same frequency as the periodic current during the initial stage and then oscillates with a double-frequency period at large time; whereas for low frequency of the oscillation D_{a} varies cyclically with a double-frequency period from the start. It is important to note that the dispersion coefficient due to the oscillatory current is much smaller than that due to the steady one. Owing to boundary absorption, D_{a} decreases for a given frequency of the periodic current. The averaged dispersion coefficient $(\overline{D}_{\mathrm{a}})$ over the period of oscillation due to the combined effect of the steady and oscillatory currents is always positive and decreases with increase in β.

The effect of boundary absorption on the mean concentration distribution causes deviations from Gaussianity. The tendency to develop positive or negative skewness depends on the differential convection and concentration distribution across the flow in the tube. It is worthwhile to mention that Gaussianity is achieved sooner for the oscillatory current than for the steady or combined shearing currents. The mean concentration distribution $C_{\mathrm{m}}(t, z)$ is almost Gaussian for $\beta = 3$ and $t > 0.15$, whereas for large reaction parameters, it tends to negative skewness. Mean concentration profiles show how much of the slug remains, how fast the slug's centre of gravity moves, and how it disperses due to shear effects.

The authors would like to express their sincere thanks to Professor P. J. Sullivan for his helpful suggestions and discussions for improvement of this paper during B.S.M.'s visit to the Department of Applied Mathematics, University of Western Ontario, Canada. The authors are also grateful to Dr Z. Mao, Department of Chemical Engineering, University of Illinois at Urbana-Champaign, for his help, and

Dr Nani G. Bhowmik, Principal Scientist of the Illinois State Water Survey for his encouragement. Many thanks also go to anonymous referees who reviewed this paper and made suggestions for its improvement.

REFERENCES

ANDERSON, D. A., TANNEHILL, J. C. & PLETCHER R. H. 1984 *Computational Fluid Mechanics and Heat Transfer*. Hemisphere.

ANDERSSON, B. & BERGLIN, T. 1981 Dispersion of laminar flow through a circular tube. *Proc. R. Soc. Lond.* A **377**, 251–268.

ARIS, R. 1956 On the dispersion of a solute in a fluid flowing through a tube. *Proc. R. Soc. Lond.* A **235**, 67–77.

ARIS, R. 1960 On the dispersion of a solute in pulsating flow through a tube. *Proc. R. Soc. Lond.* A **259**, 370–376.

BARTON, N. G. 1983 On the method of moments for solute dispersion. *J. Fluid Mech.* **126**, 205–218.

BARTON, N. G. 1984 An asymptotic theory for dispersion of reactive contaminants in parallel flow. *J. Austral. Math. Soc.* B **25**, 287–310.

BARTON, N. G. & STOKES, A. N. 1986 A computational method for shear dispersion in parallel flow. In *Computational Techniques and Applications*, CTAC-85 (ed. J. Noye & R. May), pp. 345–355. North-Holland.

CHATWIN, P. C. 1970 The approach to normality of the concentration distribution of solute in a solvent flowing along a straight pipe. *J. Fluid Mech.* **43**, 321–352.

CHATWIN, P. C. 1975 On the longitudinal dispersion of passive contaminant in oscillatory flows in tubes. *J. Fluid Mech.* **71**, 513–527.

FISCHER, H. B., LIST, E. J., KOH, R. C. Y., IMBERGER, J. & BROOKS, N. H. 1979 *Mixing in Inland and Coastal Waters*. Academic.

GILL, W. N. & ANANTHAKRISHNAN, V. 1967 Laminar dispersion in capillaries: Part 4. The slug stimulus. *AIChE J.* **13**, 801–807.

GILL, W. N., RUCKENSTEIN, E. & HSIEH, H. P. 1975 Homogeneous models for porous catalysts and tubular reactors with heterogeneous reactions. *Chem. Eng Sci.* **30**, 685–694.

GILL, W. N. & SANKARASUBRAMANIAN, R. 1970 Exact analysis of unsteady convective diffusions. *Proc. R. Soc. Lond.* A **316**, 341–350.

GUPTA, P. S. & GUPTA, A. S. 1972 Effects of homogeneous and heterogeneous reactions on the dispersion of a solute in the laminar flow between two plates. *Proc. R. Soc. Lond.* A **330**, 59–63.

GÜVEN, O., MOLZ, F. J. & MELVILLE, J. G. 1984 An analysis of dispersion in a stratified aquifer. *Wat. Resour. Res.* **20**, 1337–1354.

HOLLEY, E. R., HARLEMAN, D. R. F. & FISCHER, H. B. 1970 Dispersion in homogeneous estuary flow. *J. Hydraul. Div. ASCE* **96**, 1691–1709.

JIMENEZ, C. F. & SULLIVAN, P. J. 1984 Contaminant dispersion in some time-dependent laminar flows. *J. Fluid Mech.* **142**, 57–77.

LAPIDUS, L. & PINDER, G. F. 1982 *Numerical Solution of Partial Differential Equations in Science and Engineering*. Wiley-Interscience.

MAZUMDER, B. S. & DAS, S. K. 1989 Dispersion of contaminant in oscillatory flow through a pipe – computation of moments. *Acta Mech.* **80**, 151–156.

MEHTA, R. V., MERSON, R. L. & MCCOY, B. J. 1974 Hermite polynomial representation of chromatography elution curves. *J. Chromatogr.* **88**, 1–6.

MUKHERJEE, A. & MAZUMDER, B. S. 1988 Dispersion of contaminant in oscillatory flows. *Acta Mech.* **74**, 107–122.

OKUBO, A. 1967 The effect of shear in an oscillatory current on horizontal diffusion from an instantaneous source. *Intl J. Oceanol. Limnol.* **1**, 194–204.

PURNAMA, A. 1988 Boundary retention effects upon contaminant dispersion in parallel flows. *J. Fluid Mech.* **195**, 393–412.

PURTELL, L. P. 1981 Molecular diffusion in oscillating laminar flow in a pipe. *Phys. Fluids* **24**, 789–793.

Sankarasubramanian, R. & Gill, W. N. 1973 Unsteady convective diffusion with interphase mass transfer. *Proc. R. Soc. Lond* A **333**, 115–132.

Schlichting, H. 1966 *Boundary Layer Theory*. McGraw-Hill.

Sexl, Th. 1930 Uber den von E. G. Richardson entdeckten 'Annulareffekt.' *Z. Phys.* **61**, 349.

Smith, R. 1982 Contaminant dispersion in oscillatory flows. *J. Fluid Mech.* **114**, 379–398.

Smith, R. 1983*a* The contraction of contaminant distributions in reversing flows. *J. Fluid Mech.* **129**, 137–151.

Smith, R. 1983*b* Effects of boundary absorption upon longitudinal dispersion in shear flows. *J. Fluid Mech.* **134**, 161–177.

Taylor, G. I. 1921 Diffusion by continuous movements. *Proc. Lond. Math. Soc.* **20**, 196–211.

Taylor, G. I. 1953 Dispersion of solute matter in solvent flowing slowly through a tube. *Proc. R. Soc. Lond.* A **219**, 186–203.

Uchida, S. 1956 The pulsating viscous flow superposed on the steady laminar motion of incompressible fluid in a circular pipe. *Z. Angew. Math. Phys.* **7**, 403–422.

Valentine, E. M. & Wood, I. R. 1977 Longitudinal dispersion with dead zones. *J. Hydraul. Div. ASCE* **103**, 975–990.

Yasuda, H. 1984 Longitudinal dispersion of matter due to the shear effect of steady and oscillatory currents. *J. Fluid Mech.* **148**, 383–403.

Yasuda, H. 1989 Longitudinal dispersion of suspended particles in oscillatory currents. *J. Mar. Res.* **47**, 153–168.